THE JOURNAL OF BIOLOGICAL CHEMISTRY
Vol. 278, No. 31, Issue of August 1, pp. 28840–28848, 2003

Printed in U.S.A.

Identification of Genes Encoding Arabinosyltransferases (*SCA*) Mediating Developmental Modifications of Lipophosphoglycan Required for Sand Fly Transmission of *Leishmania major**

Received for publication, March 18, 2003, and in revised form, May 14, 2003
Published, JBC Papers in Press, May 15, 2003, DOI 10.1074/jbc.M302728200

Deborah E. Dobson‡§, Brenda J. Mengeling¶, Salvatore Cilmi‖, Suzanne Hickerson‡, Salvatore J. Turco¶, and Stephen M. Beverley‡‖

From the ‡Department of Molecular Microbiology, Washington University School of Medicine, St. Louis, Missouri 63110, the ¶Department of Biochemistry, University of Kentucky Medical Center, Lexington, Kentucky 40536, and the ‖Department of Biological Chemistry and Molecular Pharmacology, Harvard Medical School, Boston, Massachusetts 02115

At key steps in the infectious cycle pathogens must adhere to target cells, but at other times detachment is required for transmission. During sand fly infections by the protozoan parasite *Leishmania major*, binding of replicating promastigotes is mediated by galactosyl side chain (scGal) modifications of phosphoglycan repeats of the major surface adhesin, lipophosphoglycan (LPG). Release is mediated by arabinosyl (Ara) capping of LPG scβGal residues upon differentiation to the infective metacyclic stage. We used intraspecific polymorphisms of LPG structure to develop a genetic strategy leading to the identification of two genes (*SCA1/2*) mediating scAra capping. These LPG side chain β1,2-arabinosyltransferases (scβAraTs) exhibit canonical glycosyltransferase motifs, and their overexpression leads to elevated microsomal scβAraT activity. Although the level of scAra caps is maximal in metacyclic parasites, scβAraT activity is maximal in log phase cells. Because quantitative immunolocalization studies suggest this is not mediated by sequestration of SCA scβAraTs away from the Golgi apparatus during log phase, regulation of activated Ara precursors may control LPG arabinosylation *in vivo*. The *SCA* genes define a new family of eukaryotic βAraTs and represent novel developmentally regulated LPG-modifying activities identified in *Leishmania*.

The trypanosomatid protozoan parasite *Leishmania* causes a spectrum of diseases, ranging from mild cutaneous lesions to fatal visceral infections, that affect over 12 million people worldwide (1). *Leishmania* is transmitted to a new vertebrate host by an insect vector, phlebotomine sand flies. When a sand fly bites an infected host, *Leishmania* amastigotes residing within the acidified phagosomes of macrophages are taken up and the blood meal enclosed by a midgut peritrophic matrix for several days, during which time parasites differentiate into the replicating procyclic promastigote stage. Several studies have emphasized the importance of the abundant promastigote surface glycolipid lipophosphoglycan (LPG)[1] and other phosphoglycans (PGs) for parasite survival in the hydrolytic environment of the sand fly midgut (reviewed in Refs. 2–4). Once the matrix is degraded, *Leishmania* promastigotes bind to midgut epithelium through an LPG-dependent interaction, to avoid being excreted with the remnants of the digested blood meal (5). As the sand fly prepares to feed again, parasites differentiate into the infectious metacyclic stage that synthesize a developmentally regulated, structurally distinct LPG that is unable to bind the midgut (5–7) and is adapted for transmission and survival in a new vertebrate host (8). The ability of *Leishmania* to alter their surface coat to ensure survival in both their insect vectors and vertebrate hosts is a common theme shared by many protozoan parasites (9).

The backbone structure of LPG is highly conserved among all *Leishmania*, consisting of a 1-*O*-alkyl-2-*lyso*-phosphatidylinositol lipid anchor and heptasaccharide core joined to a phosphoglycan (PG) polymer of 15–30 (Galβ1,4Manα1-PO$_4$) repeat units, terminated by an oligosaccharide cap (see Fig. 1). However, a number of modifications to this basic "backbone" structure have been found in different *Leishmania* strains and species, including a variety of oligosaccharide modifications of the PG repeats, the number of PG repeats, and the composition of the terminal oligosaccharide cap. Moreover, these modifications vary in different developmental stages, in a way that contributes to the stage-specific binding and release of the parasite during its infectious cycle in the fly (reviewed in Refs. 2–4, 10). For example, the ability of *Leishmania major* Friedlin V1 strain (LmFV1) parasites to establish and maintain infection in its natural vector *Phlebotomus papatasi* is facilitated by terminal β1,3-Gal side chains (scβGal) on LPG PG repeats, which bind midgut lectins (see Fig. 1*B*), and species or *L. major* mutants that lack LPG scβGal do not bind to and cannot be transmitted by *P. papatasi* (11–13). During metacyclogenesis of LmFV1, the LPG PG repeat number increases and scβGal residues are capped with β1,2-arabinose (βAra) to block midgut binding and favor parasite release (Fig. 1*B*) (6, 7). In contrast, adhesion of *Leishmania donovani* in its natural vector *Phlebotomus argentipes* is mediated by a galactosylated terminal cap in procyclic promastigote LPG, whereas in metacyclic parasites conformational changes arising from increasing LPG

* This work was supported by National Institutes of Health grants (to S. J. T. and S. M. B.). The costs of publication of this article were defrayed in part by the payment of page charges. This article must therefore be hereby marked "*advertisement*" in accordance with 18 U.S.C. Section 1734 solely to indicate this fact.

The nucleotide sequence(s) reported in this paper has been submitted to the GenBank™/EBI Data Bank with accession number(s) AY230143.

§ To whom correspondence should be addressed: Dept. of Molecular Microbiology, Washington University School of Medicine, 660 S. Euclid Ave., Box 8230, St. Louis, MO 63110. Tel.: 314-747-2631; Fax: 314-747-2634; E-mail: dedobson@borcim.wustl.edu.

[1] The abbreviations used are: LPG, lipophosphoglycan; PG, phosphoglycan; LmFV1, *L. major* strain Friedlin V1; FACE, fluorophore-assisted carbohydrate electrophoresis; scGal, galactosyl side chain; scAra, arabinosyl side chain; ORF, open reading frame; PIPES, 1,4-piperazinediethanesulfonic acid; Tn, transposon; TM, transmembrane; GFP, green fluorescent protein; nt, nucleotide(s).

length mask the LPG cap and allow parasites to be released (13). These data suggest that LPG acts as both a stage- and species-specific adhesin in the sand fly and that each parasite species has adapted its repertoire of LPG modifications for its particular sand fly vector species (2, 3).

LPG modifications that accompany LmFV1 metacyclogenesis *in vivo* are replicated in procyclic promastigotes cultures *in vitro*, during the transition from logarithmic to stationary growth phase (6, 7, 14, 15). This provides an experimentally convenient setting in which to pursue the identification of genes associated with this key developmental step. In this study we focused on the functional identification of genes participating in the stage-specific attachment of βAra to LPG scβGal, because of their importance in parasite transmission in the well-characterized *L. major-P. papatasi* model (see Fig. 1). Previously we identified genes affecting synthesis of the conserved LPG backbone using transfection-based functional rescue of LPG-deficient mutants (16–19). More recently, we have used cross-species transfection approaches to identify a constitutively expressed *L. major* gene family (*SCG*) that mediates LPG scβGal addition (20). Here we used "cross-strain" transfection to identify loci that mediate Ara capping of LPG scβGal during metacyclogenesis. The *SCA* (side chain Ara) genes encoding eukaryotic βAraTs represent important developmental genes mediating LPG structural changes necessary for parasite transmission from the sand fly to the mammalian host.

EXPERIMENTAL PROCEDURES

Leishmania Culture and Transfection—*L. major* strain Friedlin V1 (LmFV1) is a virulent clonal derivative of the Friedlin line (MHOM/IL/80/Friedlin) obtained from D. L. Sacks (National Institutes of Health). *L. major* strain LV39 clone 5 (LmLV39) is a virulent clonal derivative of the LV39 strain (MRHO/SU/59/P) obtained from R. Titus (Colorado State University). Cells were grown in M199 medium at 26 °C containing 10% heat-inactivated fetal bovine serum (21). Metacyclic promastigotes were isolated by the peanut agglutinin method (22) from cultures that had been in stationary growth phase for 2–3 days. Infections of BALB/c mice and recovery and purification of lesion amastigotes were performed as described previously (23).

Parasites were transfected by electroporation, and clonal lines were obtained by plating on semisolid M199 media (21), containing drugs appropriate for each selective marker (50 μg/ml hygromycin B and 15 μg/ml G418). Agglutination assays were performed using 3F12 monoclonal antibodies, which recognize the LPG [Ara(β1,2)Gal(β1,3)$_{1,2}$-PG repeat unit] epitope (24, 25).

Cosmid Library Transfection and 3F12 Monoclonal Antibody Panning—These studies were approved by the relevant institutional biosafety committees. An LmFV1 genomic DNA library constructed in the cosmid shuttle vector cLHYG (strain B890 (24)) was introduced by electroporation into LmLV39: 8600 independent transfectants were obtained, providing about 7-fold coverage of the *Leishmania* genome. Colonies were combined into three independent pools, and stationary phase transfectants bearing βAra-capped scβGal-modified LPG PG repeats were isolated by antibody panning using 3F12 antibody and plates coated with goat anti-mouse IgG (17, 20, 25, 26). Three successive rounds of 3F12 antibody panning were performed, yielding a strongly reactive population. Parasites were plated to isolate individual colonies, and cosmid DNAs encoding the *SCA1* locus (B2015, B2037, and B2016) or *SCA2* locus (B2017 and B2039) were recovered by transformation of *Escherichia coli* (24).

Molecular Constructs—A 6.5-kb *Bam*HI-*Hin*dIII fragment from *SCA1*$_{FV1}$ cosmid B2015 (Fig. 2) was inserted into *Bam*HI+*Hin*dIII-digested pSNBR (27), yielding pSNBR-*SCA1*$_{FV1}$ (B2350). The corresponding fragments from *SCA2*$_{FV1}$ cosmid B2017 was used to construct pSNBR-*SCA2*$_{FV1}$ (B3658). The 2.9-kb *Eco*NI-*Dra*III fragment from pSNBR-*SCA* $_{FV1}$ containing the entire predicted *SCA1*$_{FV1}$ open reading frame (ORF) plus 423 bp of 3′ flanking DNA (Fig. 4) was inserted by blunt end cloning into the *Xma*I site of pXG (B1288; (28) to yield pXG-*SCA1*$_{FV1}$ (B3965). Relevant sequence of all constructs was verified using standard methods with an Applied Biosystems ABI-373 automated DNA sequencer.

Construction and Detection of SCA1$_{FV1}$*/GFP Fusions*—An N-terminal fusion to a modified green fluorescent protein (GFP+2) was made by inserting the 2.9-kb *Eco*NI-*Dra*III fragment from pXG-*SCA1*$_{FV1}$, after addition of *Bam*HI linkers, into the B*gl*II site of pXG-GFP+2′ (B2997) to generate the sense construct pXG-*GFPSCA1*$_{FV1}$ (B3959) and the antisense construct pXG-*GFP1ACS* (B960). A C-terminal *SCA1*$_{FV1}$*GFP* fusion was made by PCR amplification of a *SCA1*$_{FV1}$ ORF lacking a stop codon using appropriate primers (B856 forward primer: 5′-ggaagatctccaccATGAGGGGGGACATCACAGCGT; B857 reverse primer: 5′-ggaagatctcagtggtggtggtggtggggcccGTATAAGCCCGTGTAAAACGA; *Leishmania* sequences are capitalized) and pXG-*SCA1*$_{FV1}$ template. This fragment was digested with *Bgl*II and *Apa*I, and blunt ends were generated by T4 DNA polymerase and ligated to *Bam*HI linkers. After *Bam*HI digestion, this fragment was cloned into the *Bam*HI site of pXG-′GFP+ (B4394 (28)) to generate pXG-*SCA1*$_{FV1}$*GFP* (B3964).

Microscopy—For fluorescence microscopy, live parasites were incubated with Hoechst 33342 to visualize nuclear and kinetoplast DNAs, fixed in 4% formaldehyde/phosphate-buffered saline, and photographed using an Olympus AX70 photomicrographic system. For immunoelectron microscopy, parasites were fixed in 4% paraformaldehyde/0.2% glutaraldehyde in 100 mM PIPES/0.5 mM $MgCl_2$, pH 7.2, for 1 h at 4 °C. Fixed parasites were embedded in 10% gelatin and infiltrated overnight with 2.3 M sucrose/20% polyvinyl pyrrolidone in PIPES/$MgCl_2$ at 4 °C. Samples were trimmed, frozen in liquid nitrogen, and sectioned with a Leica Ultracut UCT cryo-ultramicrotome (Leica Microsystems Inc.). 70-nm sections were blocked with 5% fetal bovine serum/5% normal goat serum (blocking buffer) for 30 min and subsequently incubated with rabbit anti-MBPGFP IgG (provided by E. Handman, Walter and Eliza Hall Institute, Australia) for 1 h. After washing with blocking buffer for 20 min, samples were probed with 18-nm colloidal gold-conjugated goat anti-rabbit IgG secondary antibody for 1 h. Parallel controls omitting the primary antibody were consistently negative under these conditions. Sections were washed in 100 mM PIPES buffer followed by a water rinse and stained with 0.3% uranyl acetate/2% polyvinyl alcohol. Samples were viewed with a 1200EX transmission electron microscope (JEOL).

In Vitro Transposon Mutagenesis and DNA Sequencing—pSNBR-*SCA1*$_{FV1}$ was used as a target for TyK transposon (Tn) mutagenesis (29). A total of 120 transposon insertions were mapped, and 20 that fell within the *Leishmania* insert were transfected into LmLV39. Complete double-stranded DNA sequences were obtained for the 3.2-kb *SCA1*$_{FV1}$ region (GenBank™ AY230143) using Sequenase (USB) or Taquenase (Amersham Biosciences) and appropriate TyK-specific and *SCA*-specific oligonucleotide primers (29).

RNA Analyses—Total *Leishmania* RNAs were prepared using the Trizol method (Invitrogen), and 5-μg samples were analyzed by Northern blotting (30), using a radiolabeled *Eco*NI-*Kpn*I fragment containing the *SCA1*$_{FV1}$ ORF (Fig. 4). cDNA was prepared using 1 μg of *Leishmania* total RNA and Superscript reverse transcriptase (Invitrogen) in a 20-μl reaction volume, following the manufacturer's directions. PCR reactions (20 μl), containing 1 μl of cDNA, 10 pmol each of *L. major* miniexon (B936, 5′-AACGCTATATAAGTATCAGTTCTGTACTTTA) and *SCA*-specific (B451, 5′-TGCGGCACACCATAGCAGTC or B453, 5′-CGAAGGTCCTTGCTGTGAG) primers, 0.25 mM dNTPs, and 1 unit of *Taq* polymerase (Roche Applied Science) were performed in a PTC-200 thermocycler (MJ Research) using 60 °C annealing temperature and 1.5-min elongation time for a total of 35 cycles. Products were analyzed by electrophoresis in 1.5% agarose, 1× TEA (40 mM Tris acetate, 1 mM EDTA, pH 8) gels.

Purification and Analysis of LPG—For [^{3}H]Ara metabolic labeling of LPG and βAraT assays, cells that had been in stationary growth phase for 1 day (2–4 × 10^7 cells/ml) were collected by centrifugation and resuspended at 2 × 10^9 cells/ml in fresh medium. Parasites were metabolically labeled with D-[^{3}H]Ara (25 μCi/2 × 10^9 cells in 1 ml, 15 Ci/mmol) for 6 h in fresh medium at 26 °C. The pH was adjusted to neutral by dropwise addition of saturated sodium bicarbonate after 1–2 h. LPG was extracted and purified by phenyl-Sepharose chromatography (31). LPG PG repeats were generated by hydrolysis under mild acid conditions (0.02 N HCl, 15 min at 60 °C), dephosphorylated with *E. coli* alkaline phosphatase (5 unit/ml, 16 h at 37 °C), and separated by descending paper chromatography with a solvent system consisting of *n*-butanol:pyridine:water (6:4:3, v/v) (12, 31). Aliquots of dephosphorylated PG repeats were fluorophore labeled at the reducing ends with 8-aminonaphthalene-1,3,6-trisulfate and analyzed by fluorophore-assisted carbohydrate electrophoresis (FACE) according to manufacturer's specifications (Glyko Inc., Novato, CA). When [^{3}H]Ara-labeled PG repeats (50,000 cpm) were included, gels were visualized by UV illumination, and the radioactivity eluted from excised bands was measured by scintillation counting. In some studies PG repeats were treated with *E. coli* β-galactosidase (10 units/ml, 16 h at 37 °C (32)) before labeling

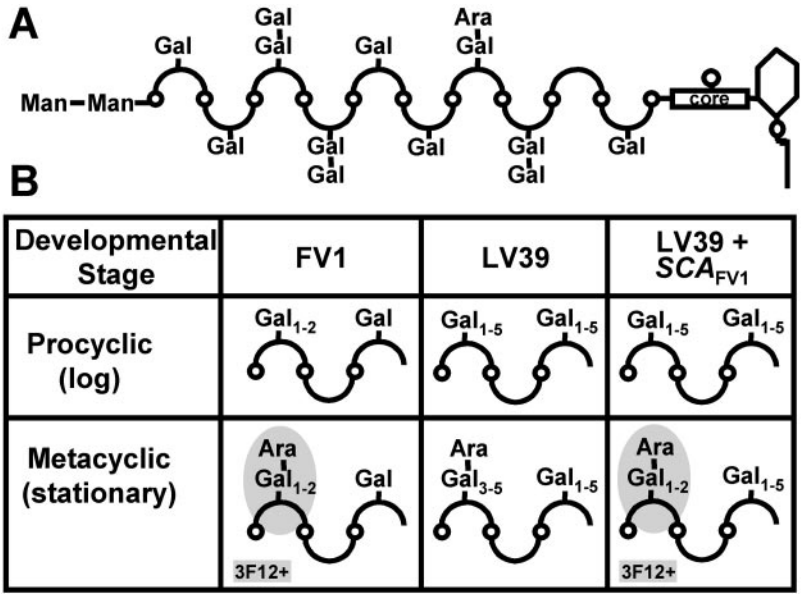

FIG. 1. **LPG PG repeat structures in *L. major* strains Friedlin V1 (FV1) and LV39 (LV39), and SCA transfectants of LmLV39 (LV39 + SCA$_{FV1}$).** *A*, LmFV1 procyclic LPG molecule. The structure shown is modified from McConville *et al.* (7). The disaccharide phosphate (PG) repeat backbone Gal(β1,4)Man(α1-PO$_4$)→6 is represented by (*circle with curved line*). On PG repeats, Gal side chain sugars are in β1,3-linkage, and Ara side chain sugars are in β1,2-linkage (10, 48). The structure of the glycan core (*box*) is Gal(α1,6)Gal(α1,3)Gal$_f$(β1,3)[Glc(α1-PO$_4$)→6]Man(α1,3)Man(α1,4)GlcN(α1,6) and is linked to a 1-*O*-alkyl-2-*lyso*-phosphatidylinositol anchor. *B*, developmental changes in LPG side chain structures. Summary of the structure of LPG PG repeat side chains from procyclic (log phase) and metacyclic (stationary phase) promastigotes (from Re. 7, Fig. 6, and data not shown). Only representative PG repeats are shown. Structures observed in LmLV39 pXG-*SCA*1$_{FV1}$ transfectants (Fig. 6) are shown. 3F12 antibody reactivity is noted, and the 3F12 epitope (Ara-Gal$_{1-2}$-PG repeat) is *shaded*.

for FACE analysis (12). Migration distances were compared with oligosaccharide standards. Strong acid hydrolysis followed by monosaccharide analysis of PG repeats indicated that the radiolabel remained as D-[^{3}H]Ara (data not shown).

LPG Glycosyltransferase Assays—Microsomes were prepared as described (12) from log or stationary growth phase parasites. β1,2-Arabinosyltransferase (scβAraT) assays were performed using microsomes (1 mg of protein), 3 μM GDP-[^{3}H]Ara, and purified LmFV1 log phase LPG (10 μg) as an exogenous acceptor (32), because it contains Gal side chains with minimal βAra capping (Fig. 1*B*). β1,3-Galactosyltransferase (scβGalT) assays were performed using microsomes (1 mg of protein), 6 μM UDP-[^{3}H]Gal, and 10 μg of purified *L. donovani* LPG, which lacks Gal side chains (12, 33). Incorporation of radiolabel into LPG was quantitated by liquid scintillation counting (12, 34).

RESULTS

Functional Identification of Genes Mediating LPG Side Chain Ara Capping—In *L. major* strain FV1 (LmFV1) procyclic promastigotes, LPG PG repeats typically contain one to two β1,3-Gal side chains (scβGal) that become further modified by β1,2-linked arabinose caps (scβAra) as parasites differentiate to the infectious metacyclic form in stationary growth phase (Fig. 1*B*). These metacyclic/stationary phase scβAra-capped PG repeats are reactive with the monoclonal antibody 3F12 (25, 26), whereas procyclic/log phase promastigotes are 3F12-unreactive (Fig. 1*B*). In contrast to LmFV1, metacyclic/stationary phase parasites of *L. major* strain LV39c5 (LmLV39) remained unreactive with 3F12 (Fig. 1*B*). Although the structure of LmLV39 LPG was unknown initially, we reasoned that expression of the LmFV1 LPG side chain capping β1,2-Ara transferase (scβAraT) would confer 3F12 reactivity in metacyclic/stationary phase LmLV39 transfectants (Fig. 1*B*).

An LmFV1 genomic library, prepared in the *Leishmania* shuttle cosmid vector cLHYG (24), was transfected into LmLV39, yielding 8600 independent transfectants. Transfectant pools were grown to stationary phase, and 3F12-reactive transfectants were recovered by 3F12 antibody panning; after three rounds, a strongly 3F12-reactive population emerged. Clonal lines were obtained by plating, and from 36 we recovered 5 different cosmids that conferred 3F12 reactivity upon retransfection into LmLV39 (Fig. 2). As for wild-type LmFV1, 3F12 reactivity was only observed when LmLV39 transfectants entered stationary phase. Restriction mapping showed these cosmids represented two loci that we named *SCA* (side chain Ara): *SCA1*$_{FV1}$ (cosmids B2015, B2016, and B2037) and *SCA2*$_{FV1}$ (cosmids B2017 and B2039). Further mapping and Southern blotting showed that these cosmid loci overlapped (Fig. 2 and data not shown), a conclusion that was recently confirmed by DNA sequencing of this chromosomal region (GenBank™ accession numbers AC087161 and AC084317).[2] Within each locus a large (13.7 kb) region showed similar restriction maps, which we termed the *SCA* conserved region (Fig. 2, *gray box*), and these were separated by 5.9 kb (Fig. 2).[2]

Identification of SCA$_{FV1}$ Genes—The active gene within *SCA*1$_{FV1}$ cosmid B2015 was localized by 3F12 reactivity tests of LmLV39 transfectants bearing either deletion derivatives or following transposon (Tn) insertion mutagenesis (Fig. 3 and 4 and data not shown). Analysis of five *SCA1*$_{FV1}$/B2015 deletions identified a 6.5-kb region that conferred 3F12 reactivity (Fig. 3), again only in stationary phase transfectants. LmLV39 transfectants bearing this 6.5-kb *SCA1*$_{FV1}$ fragment inserted in the *Leishmania* shuttle vector pSNBR (27) similarly showed stationary phase-specific 3F12 reactivity (pSNBR-*SCA1*, Fig. 3), as did an analogous pSNBR construct containing the 6.5-kb *SCA2*$_{FV1}$ fragment (pSNBR-*SCA2*, Fig. 3).

Analysis of twenty Tn insertions within the pSNBR-*SCA1*$_{FV1}$ insert showed four had lost 3F12 reactivity (Tns 38, 5, 105, and 9; Fig. 4 and data not shown). These Tn insertions clustered in a 2-kb region, and we obtained the DNA sequence out to the nearest flanking sites retaining 3F12 reactivity (Tns 120 and 30; Fig. 4; GenBank™ AY230143). This revealed a 2.5-kb open reading frame (ORF) encoding an 832-amino acid protein (Figs. 4 and 5). Expression of the predicted *SCA1*$_{FV1}$ ORF alone in the constitutive *Leishmania* expression vector

[2] P. J. Myler, E. Sisk, J. Ruiz, P. Cosenza, A. Cruz, K. Stuart, D. E. Dobson, and S. M. Beverley, manuscript in preparation.

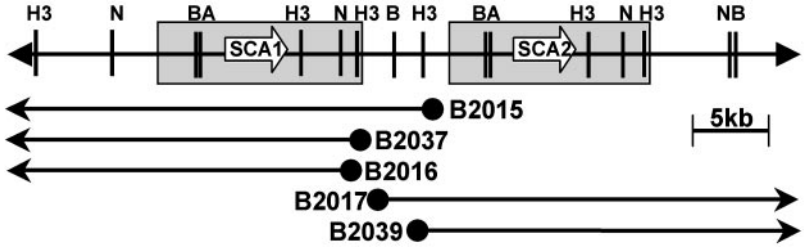

FIG. 2. **Map of the *SCA* loci in LmFV1.** Symbols are: *A*, *Asc*I; *B*, *Bam*HI; *H3*, *Hin*dIII; *N*, *Nhe*I; *filled circles*, the ends of the *Leishmania* DNA insert within each cosmid; and *arrows*, the remaining region for each cosmid. The open reading frames (ORFs) encoding *SCA1* and *SCA*2 are depicted as *open arrows* designating N to C termini. The 13.7-kb *SCA* homology region shared by *SCA*1 and *SCA*2 is *shaded*. Stationary phase LmLV39 transfectants expressing the indicated *SCA* cosmids all reacted strongly with 3F12 antibodies, whereas log phase cultures were unreactive. At least two independent transfectants were tested for each construct listed.

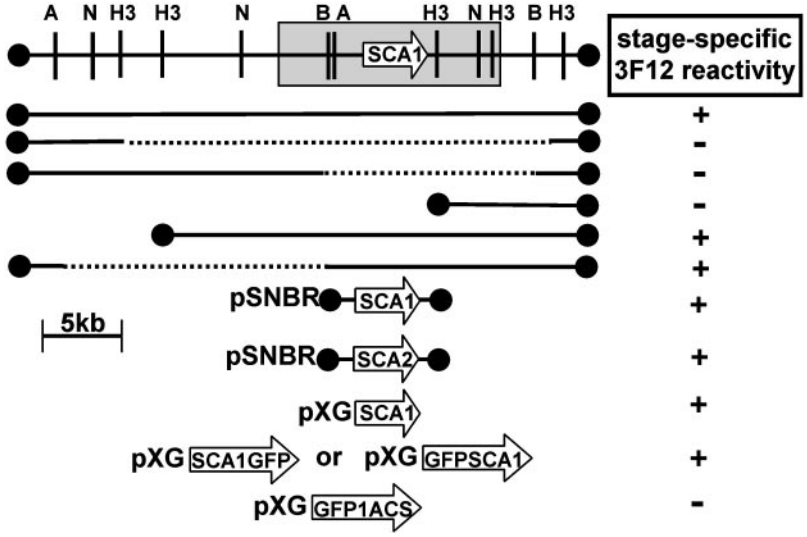

FIG. 3. **Localization of $SCA1_{FV1}$ in cosmid B2015.** The complete *Leishmania* insert is shown; map features are described in Fig. 2. Cosmid deletions used to localize the $SCA1_{FV1}$ gene are shown with *dotted lines* representing the deleted region. The active 6.5-kb *Bam*HI-*Hin*dIII (*B-H3*) fragment from cosmid B2015 ($SCA1_{FV1}$) or the homologous region from the $SCA2_{FV1}$ cosmid B2017 ($SCA2_{FV1}$) were cloned into the *Leishmania* shuttle vector pSNBR (27) to generate pSNBR-*SCA1* and pSNBR-*SCA2*, respectively. The 2.5-kb predicted $SCA1_{FV1}$ ORF and GFP-$SCA1_{FV1}$ fusion proteins (*labeled arrows*) were cloned into the *Leishmania* expression vector pXG (28) to generate pXG-*SCA1*, pXG-*SCA1GFP*, and pXG-*GFPSCA1,* respectively; antisense *SCA*1 (1ACS) was fused to GFP to generate pXG-GFP1ACS. Transfectants were scored for reactivity with 3F12 antibodies; none were reactive in logarithmic growth phase, and those reactive in stationary phase are marked with a "+."

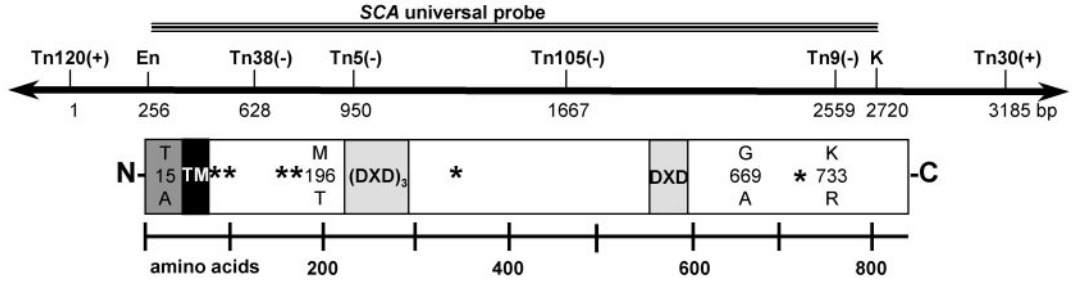

FIG. 4. **Identification and properties of $SCA1_{FV1}$.** The active $SCA1_{FV1}$ gene was localized by transposon mutagenesis of pSNBR-$SCA1_{FV1}$ (Fig. 3); the relative location of TyK transposon (*Tn*) insertion sites within a portion of pSNBR-$SCA1_{FV1}$ insert is indicated. Stationary phase-specific 3F12 reactivity of LmLV39 pSNBR-$SCA1_{FV1}$ transfectants expressing each Tn insertion construct is shown by a "+." The Tn120 insertion site was set at bp 1; the positions of *Eco*NI (*En*) and *Kpn*I (*K*) restriction sites and the "SCA universal probe" are shown. The conserved 832-amino acid SCA ORF is represented as an *open box*. Locations of the predicted cytoplasmic domain (*dark gray*), transmembrane domain (*black*), presumptive glycosyltransferase D*X*D or $(DXD)_3$ catalytic motifs, and N-glycosylation sites (*asterisks*) are noted. Differences between SCA1 and SCA2 proteins are shown with the SCA1 residue above.

pXG (pXG-$SCA1_{FV1}$) yielded 3F12-reactive LmLV39 transfectants, again showing stationary phase specificity (Fig. 3).

Properties of the Predicted $SCA1_{FV1}$ Protein—The predicted $SCA1_{FV1}$ protein contains 832 amino acids with the topology of a type II membrane protein (35), containing a single transmembrane domain (amino acids 50–72; *TM* in Fig. 4) preceded by an N-terminal signal anchor sequence of 49 amino acids (36). The $SCA1_{FV1}$ protein contained two "D*X*D" sequence motifs (DTDIDRD or "$(DXD)_3$" at amino acids 256–262, DAD at amino acids 572–574; Figs. 4 and 5), a motif common to many glycosyltransferases, which is implicated in catalytic activity (37, 38), and six potential *N*-glycosylation sites (*asterisk*, Fig. 4). This suggested that $SCA1_{FV1}$ encoded the LPG side chain β1,2-Ara transferase (scβAraT) with a luminal catalytic domain, a conclusion supported by enzymatic studies of *SCA* transfectants (below).

Similar results were obtained with $SCA2_{FV1}$ gene (GenBank™ AC087161),[2] which showed 99.8% nucleotide identity

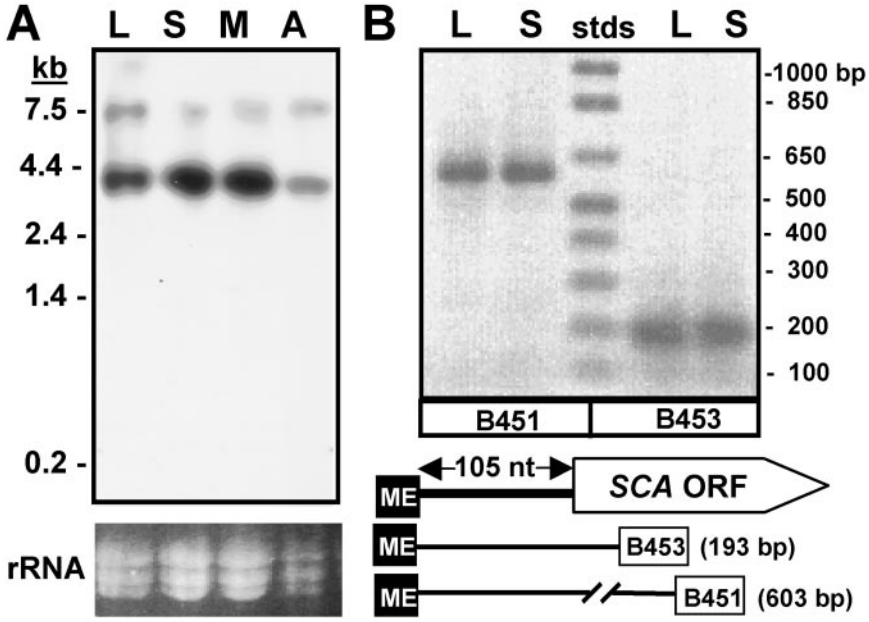

FIG. 5. **Developmental expression of *SCA* mRNA.** *A*, Northern blotting. Total RNA (5 μg) prepared from log phase (*L*), stationary phase (*S*), purified metacyclics (*M*), and amastigotes (*A*) was subjected to Northern blot analysis with a radiolabeled $SCA1_{FV1}$ "universal" probe (Fig. 4). Positions of RNA size standards are marked. Ribosomal RNA (*lower panel*) was used as a loading control. *B*, mapping 5′-end of *SCA* mRNA. cDNA was prepared from total RNA isolated from logarithmically growing LmFV1 promastigotes as described ("Experimental Procedures"). PCR reactions included *L. major* miniexon and universal SCA coding region primers B451 or B453, and products were analyzed by gel electrophoresis. Positions of DNA size standards are marked. The 105-nt SCA 5′-untranslated regions determined by RT-PCR is depicted, with the SCA ORF (*arrow*); the *black box* labeled "*ME*" represents the 39-nt miniexon added by trans-splicing to all *L. major* mRNAs. RT-PCR fragments using the indicated primers are shown (fragment size in *parentheses*).

with $SCA1_{FV1}$ (2491/2496 nt). The predicted $SCA2_{FV1}$ protein differed by four conservative amino acid replacements from $SCA1_{FV1}$ (T15A, M196T, G669A, and K733R) and retained the structural motifs seen in $SCA1_{FV1}$ (Fig. 4).

Database searches with the *SCA* genes showed 31% amino acid identity to a gene located on LmFV1 chromosome 34 emerging from the *L. major* Genome Project, and the A14 gene of *L. donovani* (GenBank™ AAK62048 (39)). These genes predict proteins of 901 or 902 amino acids with 92% amino acid identity, and we have named them *SCA*-Like (*SCAL*). Similar to SCA1/2, the predicted LmSCAL protein contains an N-terminal transmembrane domain (amino acids 71–93) and $(DXD)_3$ and D*X*D catalytic motifs at positions analogous to that seen in the SCA ORFs (DTDADCD, amino acids 300–306; DAD, amino acids 481–483). No relationships to other proteins were detected.

Structure and Developmental Expression of SCA RNA—In Northern blot analysis an $SCA1_{FV1}$ ORF probe (Fig. 4) identified a 3.5-kb mRNA in log phase LmFV1 cells, with lower amounts of a 7.5-kb mRNA (Fig. 5*A*). Because *SCA1* and *SCA2* exhibit 99.8% nucleotide identity across the predicted mRNA coding region, it is likely that the longer mRNA represents a processing intermediate arising from normal polycistronic transcription, which is often seen in trypanosomatids. The 5′-end of the *SCA* transcripts was mapped by RT-PCR to a position 105 nt upstream of the predicted SCA protein start site (Fig. 5*B*). *SCA* transcript levels increased 3- to 4-fold in stationary phase and metacyclic parasites (Fig. 5*A*), concurrently with the increased βAra-capping of LPG Gal side chains in this stage (Figs. 1*B* and 6). In lesion amastigotes *SCA* mRNA levels declined about 10-fold relative to metacyclic/stationary phase parasites (Fig. 5*A*), paralleling the shutdown of LPG synthesis in this stage (40).

Analyses of LPG Structure in Wild-type and SCA-transfected Parasites—Stationary phase parasites were metabolically labeled with [^{3}H]Ara, and the structure of purified LPG PG repeats was analyzed by descending paper chromatography ("Experimental Procedures," Fig. 6*A*). Stationary phase LmFV1 LPG PG repeats contained primarily [Ara-Gal] side chain modifications, as expected (Fig. 6*A*) (7). Stationary phase LmLV39 LPG also yielded Ara-labeled PG repeats, but with a decreased mobility suggestive of increased Gal side chain length (Fig. 6*A*); as shown below, this is due to the occurrence of oligo(β1,3)Gal side chains in LmLV39 LPG. Notably, stationary phase LmLV39 parasites lacked significant levels of the [Ara-Gal_{1-2}]-modified PG repeats, the epitope recognized by the 3F12 antibody (26), whereas the 3F12-reactive stationary phase LmLV39 pXG-$SCA1_{FV1}$ transfectants showed high levels of [Ara-Gal_{1-2}]-modified PG repeats (Fig. 6*A*).

The structures of the [^{3}H]Ara-labeled LPG PG repeats were analyzed by fluorophore labeling and electrophoretic separation, followed by visualization of fluorescence and liquid scintillation counting of gel slices (Fig. 6*B* and data not shown). Stationary phase LmFV1 LPG PG repeats exhibited the expected pattern, corresponding to [Gal-, Ara-Gal-, Gal_2-, and Ara-Gal_2]-modified PG repeats (Fig. 6*B*, *lane 4*; bands with *stars* indicate bands labeled by Ara; data not shown). βGal-terminated repeats were susceptible to digestion with β-galactosidase, whereas βAra-terminated repeats were resistant (Fig. 6*B*, *lane 5*). In contrast, LmLV39 LPG PG repeats exhibited a more complex pattern. Most of these bands were susceptible to digestion with β-galactosidase, showing they contained oligo-βGal side chains (Fig. 6*B*, *lane 2*). Several of the bands contained Ara caps, because they were resistant to β-galactosidase and labeled with Ara (Fig. 6*B*, *lane 3*; the Ara-containing bands are *starred*, but levels were below that detectable by UV illumination; data not shown). Interestingly, although LmLV39 PG repeats containing Gal_{1-2} side chains were abundant, Ara capping of these was not observed. Thus as summarized in Fig. 1*B*, LPG PG repeats in stationary phase LmLV39 contained a range of oligo-βGal modifications (to more than 5 residues; Fig. 6*B*), but Ara caps were found only on some of the longer oligo-

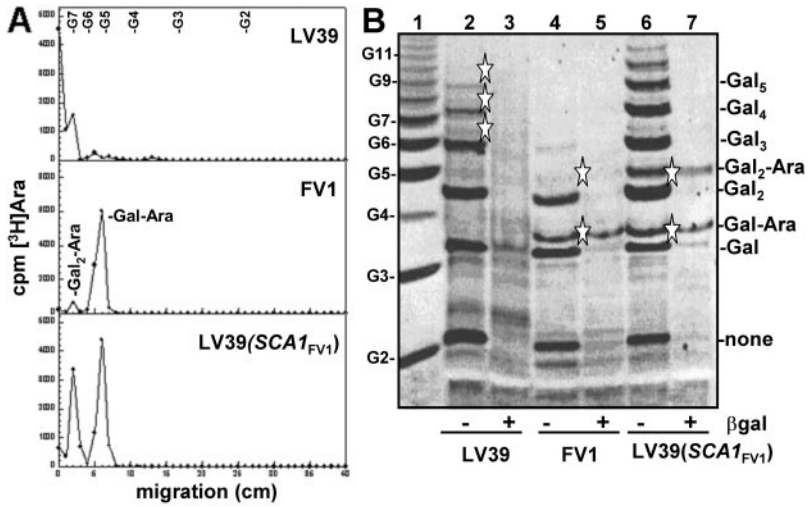

FIG. 6. **Analysis of LPG PG repeat structures.** *A*, [^{3}H]Ara metabolic labeling of *L. major* LPG repeats. Stationary phase parasites from LmFV1 (FV1), LmLV39 (LV39), or LmLV39 pXG-*SCA1*$_{FV1}$ transfectants (LV39 *SCA1*$_{FV1}$) were metabolically labeled with [^{3}H]Ara, processed, and analyzed by descending paper chromatography as described under "Experimental Procedures." The chromatogram was cut into 1-cm segments, and [^{3}H]Ara was quantitated by liquid scintillation counting. Migration of glucose oligomer standards composed of 2–7 residues (*G2–G7*) is marked. *B*, fluorophore-assisted carbohydrate electrophoresis (FACE) analysis of *L. major* LPG repeats. Dephosphorylated LPG PG repeats generated from the *L. major* lines described in *panel A* were incubated in the presence (+) or absence (−) of *E. coli* β-galactosidase (*βgal*) and subjected to FACE analysis. Only PG repeats containing βGal side chains capped with β1,2-Ara remain after β-galactosidase digestion. After UV visualization, bands were excised from the gel, and radioactivity was measured by scintillation counting. An *open star* denotes repeats containing D-[^{3}H]Ara. LPG side chain structures corresponding to each major band are noted on the *right*; "*none*" refers to unsubstituted PG repeat. *Lane 1*, glucose oligomer standards (*G2–G11*), as described in *panel A*.

βGal-modified repeats. Log phase LmLV39 LPG also contained oligo-βGal-modified PG repeats, without Ara caps (data not shown; Fig. 1*B*), and thus the oligo-βGal LPG side-chain modifications reflect strain rather than developmental stage differences.

LPG PG repeats from stationary phase LmLV39 pXG-*SCA1*$_{FV1}$ transfectants exhibited a hybrid pattern. These transfectants retained the oligo-βGal side chains found in LmLV39, as shown by their susceptibility to β-galactosidase and lack of Ara labeling (Fig. 6*B*, *lanes 6* and *7*). Additionally they possessed new bands whose mobility, β-galactosidase resistance, and Ara incorporation properties were identical to LmFV1 LPG PG repeats containing [Ara-Gal] and [Ara-Gal$_2$] side chains (Fig. 6*B*, compare *lanes 6–7* with *lanes 4–5*). This was consistent with the data shown in Fig. 6*A* and the 3F12 reactivity of these cells. In log phase, LmLV39 pXG-*SCA1*$_{FV1}$ transfectants were identical to the LmLV39 parent, exhibiting oligo-βGal side chains (to more than 5 residues, Fig. 1*B* and data not shown).

SCA Overexpression Specifically Increases Stage-specific Side Chain β1,2-Arabinosyltransferase (scβAraT) Activity—We used an *in vitro* assay to measure LPG-dependent scβAraT activity, incubating stationary phase parasite microsomes with the nucleotide sugar donor GDP-D-[^{3}H]Ara and purified log phase LmFV1 LPG acceptor and followed the transfer of D-[^{3}H]Ara to the exogenous LPG (34). Stationary phase LmFV1 microsomes showed 2.7-fold more scβAraT activity than LmLV39 microsomes (V1 = 100%, LV39 = 36.7 ± 8.3% (n = 7); Fig. 7*A*). A mixing experiment with equal amounts of LmFV1 and LmLV39 microsomes yielded an intermediate level of scβAraT activity, suggesting that the lower activity in LmLV39 parasites was not due to an endogenous inhibitor of scβAraT activity (data not shown). Significantly, stationary phase LmLV39 parasites transfected with either pSNBR-*SCA1*$_{FV1}$ or pSNBR-*SCA2*$_{FV1}$ showed significantly higher levels of scβAraT activity compared with wild type LmLV39 (2.7 ± 1.1-fold, n = 3; Fig. 7*A*).

We then assayed both LPG-dependent scβGalT and scβAraT activity in the two lines, in log and stationary phase cells. LPG PG repeat galactosylation is mediated by the activity of members of the *SCG* gene family, which collectively exhibit both initiation and elongating scβGalT activity (20). LPG scβGalT assays were conducted using microsomes, UDP-[^{3}H]Gal and log phase *L. donovani* LPG (which lacks LPG side chain modifications) (12, 20) as an exogenous acceptor. First, scβGalT activity was higher in LmLV39 than in LmFV1 in both log and stationary phase microsomes (4 ± 2.3-fold, n = 3, Fig. 7*B*), consistent with the higher degree of LPG side chain galactosylation (Fig. 6*B*). Second, in both strains scβGalT activity was 2- to 3-fold less in stationary phase compared with log phase microsomes (Fig. 7*B*). Third, microsomes derived from pXG-*SCA1*$_{FV1}$ LmLV39 transfectants showed comparable scβGalT activities to untransfected LmLV39, in both growth phases (Fig. 7*B*). These studies confirmed that stationary phase microsomes from LmFV1 had higher scβAraT activity than LmLV39, and that pXG-*SCA1*$_{FV1}$-transfected LmLV39 showed scβAraT levels comparable to that seen in LmFV1 (Fig. 7*B*). Unexpectedly, log phase scβAraT activity was 3- to 4-fold higher than that seen in stationary phase microsomes, for both LmFV1 and LmLV39 (Fig. 7*B*). This was surprising, because both *SCA* mRNA levels (Fig. 5*A*) and Ara-capping of LPG Gal side chains (Fig. 1*B*) (6, 7) increased in stationary phase.

Subcellular Localization of SCA1$_{FV1}$—The biosynthetic proteins involved in synthesis of the LPG backbone have been localized to the parasite Golgi apparatus (17, 28, 41). To localize SCA protein within the cell, we generated N- or C-terminal fusions of *SCA1*$_{FV1}$ to a GFP reporter protein in the expression vector pXG ("Experimental Procedures"). These were transfected into LmLV39, where they both conferred stationary phase-specific 3F12 reactivity (Fig. 3, pXG-*SCA1GFP*, pXG-*GFPSCA1*); in contrast, a control bearing SCA1 inserted in an antisense orientation to the GFP did not (Fig. 3, pXG-*GFP1ACS*). In stationary phase both *GFPSCA1*$_{FV1}$ transfectants showed GFP fluorescence, localized to a small region between the nucleus and kinetoplast that is the site of the parasite Golgi apparatus (Fig. 8*A* and data not shown). The GFP fluorescence intensity of *SCA1*$_{FV1}$GFP transfectants was about 5-fold lower than for *GFPSCA1*$_{FV1}$ transfectants (data

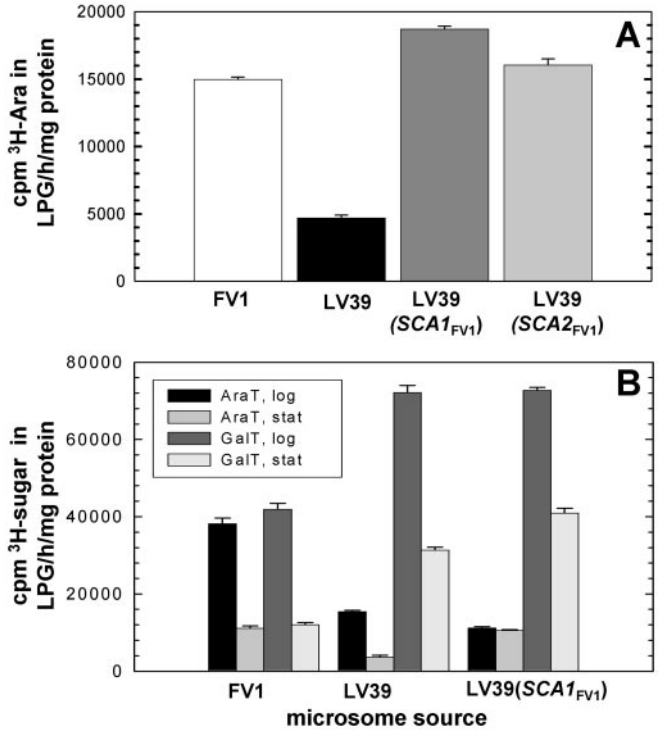

FIG. 7. **Microsomal LPG side chain glycosyltransferase activities.** *A*, stationary phase microsomal LPG side chain Ara transferase (scβAraT) activity. Microsomes prepared from stationary phase parasites were assayed for LPG-dependent scβAraT activity ("Experimental Procedures"); scβAraT activity is reported as cpm of [^{3}H]Ara transferred to exogenous LmFV1 log phase LPG/h/mg of protein. *Error bars* represent standard error of the mean for triplicate reactions. LmLV39*SCA1*$_{FV1}$ and LmLV39*SCA2*$_{FV1}$ refer to LmLV39 transfectants expressing pSNBR-*SCA1*$_{FV1}$ and pSNBR-*SCA2*$_{FV1}$ respectively. This experiment is representative of four independent experiments. *B*, comparison of LPG-dependent scβAraT and scβGalT activities in different developmental stages. Microsomal LPG-dependent scβAraT (as defined in *panel A*) and scβGalT (reported as [^{3}H]Gal transferred to exogenous *L. donovani* LPG/h/mg of protein) activities were measured as described under "Experimental Procedures," using microsomes derived from the indicated log phase or stationary phase cultures. "*LmLV39SCA1*$_{FV1}$" refers to LmLV39 transfectants expressing pXG-*SCA1*$_{FV1}$. This experiment is representative of two independent experiments.

not shown), possibly due to differences in location of the GFP tag (cytoplasmic in GFPSCA1$_{FV1}$; Golgi lumen in SCA1$_{FV1}$GFP).

As noted earlier, although the degree of LPG side-chain βAra modification increases 4- to 5-fold in stationary phase, the level of microsomal scβAraT activity was less in this stage (Figs. 1 and 7). Among the potential explanations for this, we asked whether the SCA protein showed stage-dependent localization, such that it was targeted away from Golgi apparatus in log phase and so excluded from its substrates. The localization of *SCA1GFP* fusion protein in log and stationary phase LmLV39 *GFPSCA1*$_{FV1}$ transfectants was quantitated follow cryo-immunoelectron microscopy and counting of gold particles (Fig. 8 (*B* and *C*) and Table I). These studies showed that the *SCA1GFP* fusion protein was localized to the Golgi apparatus to equivalent extents in both stages (Table I). Consistent with the activity measurements (Fig. 7*B*), the level of protein expression as judged by gold particle density was decreased in stationary phase (about 15% of log phase; Table I).

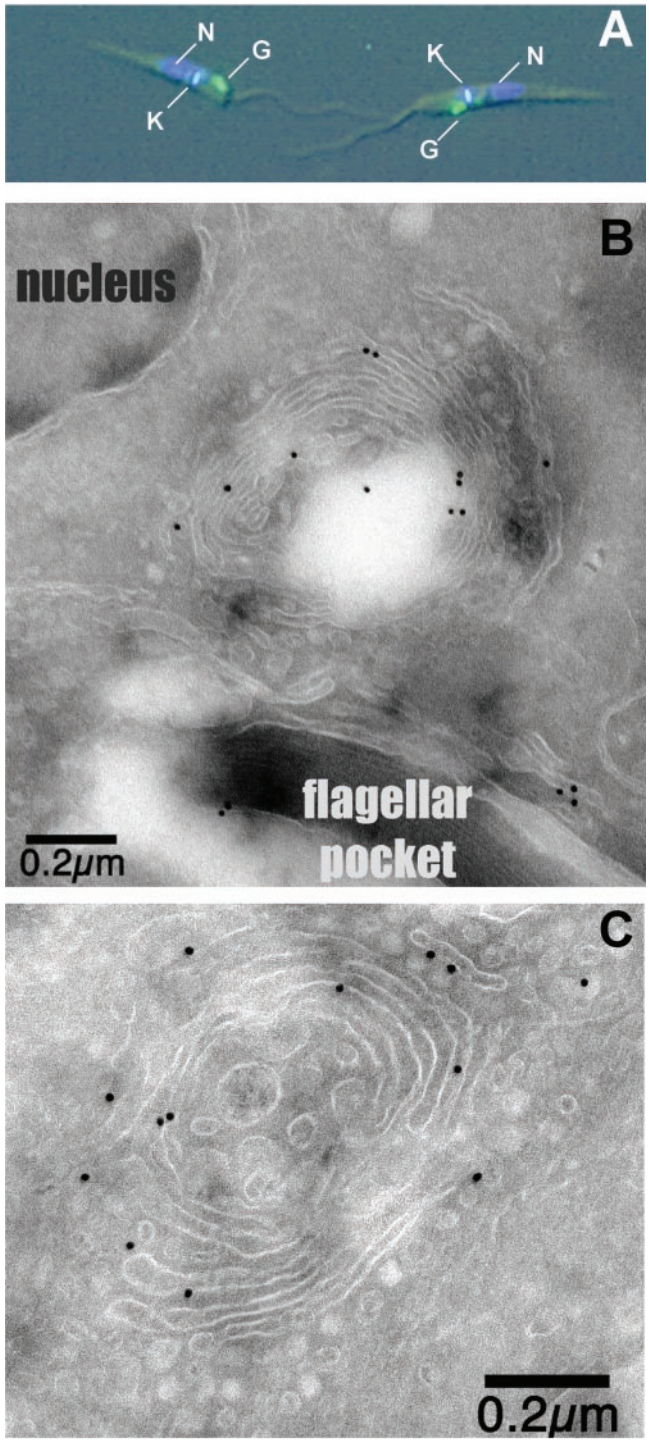

FIG. 8. **Localization of GFP*SCA*1 fusion proteins to the Golgi apparatus.** *A*, fluorescence microscopy. Stationary phase LmLV39 transfectants expressing pXG-*GFPSCA1*$_{FV1}$ were washed with phosphate-buffered saline, stained with Hoechst 33342, and analyzed by fluorescent microscopy as described ("Experimental Procedures"). Parasites were photographed using a 60× objective under conditions for detection of either GFP (*green*) or DNA (*blue* to *white*) fluorescence and then overlaid as described previously (28). *G*, Golgi apparatus; *N*, nucleus; *K*, kinetoplast. *B* and *C*, cryo-immunoelectron microscopy. Stationary phase pXG-*GFPSCA1*$_{FV1}$ LmLV39 transfectants were subjected to cryo-immunoelectronic microscopy ("Experimental Procedures"). *B*, gold particles decorating the Golgi apparatus (the flagellar pocket and nucleus are marked); *C*, the Golgi apparatus of a different cell.

DISCUSSION

We used a functional approach to identify two genes affecting βAra capping of galactosylated LPG PG repeats, *SCA*1 and *SCA*2. The predicted *SCA* proteins (Fig. 4) exhibited characteristics of LPG biosynthetic glycosyltransferases, including a type II membrane topology, "D*X*D" catalytic sequence motifs (38), and localization to the Golgi apparatus (Fig. 8). That *SCA* genes encode the glycosyltransferases themselves was shown

TABLE I
Quantitative immunoelectron microscopic localization of GFP-SCA1$_{FV1}$ to specific cellular regions in LmLV39 GFPSCA1$_{FV1}$ transfectants by binding of gold-labeled anti-GFP antisera

Parasites were prepared as described under "Experimental Procedures"; the GFP-SCA1 fusion protein was detected with anti-MBP-GFP rabbit IgG primary antibodies and colloidal gold-labeled goat-anti-rabbit IgG secondary antibodies.

Gold particles	Log phase	Stationary phase
Total in 20 cells	126	19
In Golgi (% total)	111 (88%)	12 (63%)
In flagellar pocket	0	0
In Golgi/flagellar pocket region	2	1
In other cellular locations	13	6

by expression of SCA1$_{FV1}$ or SCA2 $_{FV1}$ from episomal vectors, which resulted in increased levels of LPG-dependent scβAraT capping activity in purified microsomes and elevated levels of βAra-Gal-PG repeats in LPG isolated from stationary phase parasites (Figs. 1, 6, and 7). Preliminary studies of SCA1$_{FV1}$ protein expressed heterologously in a baculovirus system confirm this finding.[3] Notably, these enzymes define a new subfamily of glycosyltransferases, the first such eukaryotic βAraTs reported.

The two *SCA* genes are encoded by a duplicated chromosomal region encompassing 13.7 kb ("SCA conserved region" in Fig. 2), which show 99.7% nucleotide identity.[2] The predicted SCA1 and SCA2 proteins differ by only four conservative amino acid substitutions (Fig. 4), which at present seem unlikely to cause significant functional differences. Interestingly, the duplicated regions encompassing *SCA1* and *SCA2* contain six ORFs, which show strong homology (31–42% amino acid identity in the predicted luminal domain) to members of the *SCG* gene family (our GenBank^{TM} numbers (20)). We have designated these six genes surrounding *SCA1/2* as SCG related (*SCGR1–6*). *SCG* genes encode active scβGalTs that mediate galactosylation of the LPG PG repeats and thus form the substrate upon which the scβAraT-capping enzymes acts (Fig. 1) (20). The arrangement of *SCA1,2* and *SCGR1–6* raises the possibility of an LPG side-chain glycosyltransferase gene cluster, analogous to operons encoding the enzymes responsible for O antigen synthesis in bacteria (42). However, thus far we have been unable to detect LPG-modifying activity in several transfection tests of *SCGR* genes and their biological or enzymatic functions are unknown.[4]

LmLV39 Encodes a Highly Galactosylated LPG—At the time we began our studies the structure of LmLV39 LPG was unknown, necessitating its determination. The LPG of log phase LmLV39 promastigotes contains PG repeats with long scβGal polymers (ranging upwards of Gal$_5$; Fig. 6*B* and data not shown), and, accordingly, LmLV39 expresses 4-fold higher levels of LPG-dependent scβGalT activity (Fig. 7). As parasites enter stationary phase these scβGal polymers become capped with Ara residues, in a manner analogous to the process in LmFV1 (Figs. 1*B* and 7*B*). Thus the theme of LPG-mediated attachment via scβGal residues and release by Ara-capping appears to be conserved in two *L. major* strains. Recently, interactions of *L. major* with host macrophages through the Gal-binding lectin galectin-3 have been shown (43). Potentially, changes in the length and degree of LPG scβGal addition may play a role in the ability of different parasites to induce disease pathology, which can vary greatly among different *Leishmania* species and strains.

A Retrospective Analysis of the 3F12 Selection Suggests Divergence in scβAraT Specificity in Different L. major Strains—Knowledge of the structure of the LmLV39 LPG provided the opportunity to retrospectively examine the basis of our successful genetic strategy. Monoclonal antibody 3F12 was known to recognize [Ara-Gal]- and [Ara-Gal$_2$]-modified PG repeats present in LmFV1, but not PG repeats containing Ara-capped long Gal side chains (26), consistent with its lack of reactivity with LmLV39 LPG at any stage (Fig. 1*B*). Our data suggest that both quantitative and qualitative factors may have contributed to the formation of the 3F12-reactive [Ara-Gal$_{1-2}$-PG repeat] determinant in the LV39 *SCA* transfectants.

First, introduction of *SCA1* or *SCA2* on episomal vectors into LmLV39 led to an increase in LPG-dependent scβAraT activity relative to scβGalT activity in stationary phase parasites (Fig. 8). This suggests a model invoking "premature" Ara capping of LPG scβGal, thereby yielding [Ara-Gal$_{1-2}$] side chains (Figs. 1*B* and 6). However, in its simplest form, "premature capping" predicts that overexpression of the *SCA*-encoded scβAraT should result in a gradual, uniform shift in the distribution of Ara-capped PG repeats, from longer to shorter scβGal polymers. Instead, the LmLV39-*SCA1*$_{FV1}$ transfectants maintained high levels of longer oligoβGal-modified PG repeats, superimposed upon which were [Ara-Gal$_{1-2}$]-modified PG repeats. The simplest explanation is that the LmFV1 *SCA* scβAraT has a preference for short Gal side chains on PG repeats, exactly the ones present normally within LmFV1. This model is testable and makes several predictions about the relative activity of LmFV1 *versus* LmLV39 *SCA* scβAraTs with LPG acceptors showing different scβGal lengths. Recently we have identified the *SCA* locus in LmLV39, and this will enable future tests of this strain's *SCA* scβAraT activities.[5] One precedent for closely related enzymes exhibiting significant difference in LPG biosynthetic specificities are the scβGalTs encoded by the *SCG* gene family, which can show either mono- or oligo-scβGalT activity (20) .

What Controls the Level of LPG scβAra Capping?—As parasites move from log to stationary growth phase, the levels of scβAra capping of LPG Gal side chains in total cellular LPG increased in the two strains of *L. major* studied here, as do *SCA* mRNA levels (Figs. 1 and 5). Thus it was surprising to find that the levels of scβAraT activity declined in stationary phase in both strains (Fig. 7), which paralleled the decrease in protein levels seen by quantitative immunoelectron microscopy of an SCA1$_{FV1}$GFP fusion protein (Table I). Interestingly, LPG-dependent scβGalT activities showed a similar decline in these microsome preparations (Fig. 7*B*). Possibly, upon cessation of growth in stationary phase and differentiation to the smaller metacyclic stage (44), the overall demand for *de novo* synthesis of surface components may generally decline. However, this does not account for the specific 4- to 5-fold rise of Ara-capped LPG Gal side chains in stationary phase LPG.

Transfection tests showed that the *SCA1*$_{FV1}$ coding region alone was sufficient to yield stage-specific regulation when expressed from the pXG vector (Fig. 3), which gives rise to a uniform level of mRNA expression in all parasite growth phases and stages (28, 45). Potentially *in vivo*, post-translational modifications of the SCA1$_{FV1}$ protein, or the formation of larger complexes with chaperones (analogous to the interaction of the of the LPG PG backbone GalT with the LPG3 GRP94/HSP90 chaperone (17)) or other parasite glycosyltransferases, could be responsible for inhibition of Ara-capping of LPG Gal side chains in log phase parasites. However, this model requires the ad hoc assumption that these processes are dis-

[3] M. Goswami, D. E. Dobson, S. M. Beverley, and S. J. Turco, unpublished observations.

[4] D. E. Dobson, L. D. Scholtes, S. J. Turco, and S. M. Beverley, unpublished data.

[5] D. E. Dobson, A. K. Cruz, and S. Beverley, unpublished data.

rupted during preparation of microsomes suitable for *in vitro* assays.

Alternatively, *L. major* may regulate scβAra-capping of LPG Gal side chains by mechanisms other than controlling scβAraT activity. Because LPG biosynthesis occurs in the Golgi apparatus, one possibility was that *SCA* scβAraTs were sequestered in another cellular compartment, separate from the galactosylated LPG substrate in log phase. Regulated cellular compartmentalization is a common method for controlling flux in many biochemical pathways (46). We tested this by quantitative immunoelectron microscopy and showed that an $SCA1_{FV1}$GFP fusion protein, which showed proper stage-dependent activity, was localized in the Golgi apparatus in both stages and at higher levels in log phase cells. Thus stage-regulated compartmentalization appears not to occur for the *SCA* scβAraTs.

Thus we currently favor a model in which the degree of LPG scβAra capping is controlled by availability of the GDP-Ara substrate. This could occur through regulation of synthesis, presumably through the activities of an Ara-1-kinase and GDP-Ara pyrophosphorylase (47). Alternatively, transport of GDP-Ara into the Golgi apparatus could be the point of control. This nucleotide sugar is transported via the multispecific Golgi GDP-Man transporter encoded by *LPG2* (for both LPG and other PGs (18, 41)). However, we consider this unlikely since *LPG2* mRNA is expressed at higher levels in log phase *L. donovani* promastigotes (18, 41).

Notably these studies emphasize a recurrent theme emerging from the study of gene regulation in trypanosomatid protozoans, namely that mRNA levels are often poorly correlated with protein or enzymatic activity (46). The *SCA* system is a particularly remarkable example as *SCA* mRNA and protein/scβAraT activities change in opposite directions (Figs. 5 and 7 and Table I).

Functional Genetics of LPG Biosynthesis and Leishmania Differentiation—The *SCA* genes identified from *L. major* provide one tool to understand how the transition from procyclic to virulent metacyclic parasite is regulated and may provide new insights into *Leishmania* virulence and potential ways to control transmission from its sand fly host. Because Ara has not been found in mammalian glycoconjugates, the presence of Ara-capped LPG on infective metacyclic parasites could serve as a target for a transmission-blocking vaccine. In this scenario, antibodies elicited by β(1,2)Ara-terminating-βGal oligosaccharides, which are easily synthesized and likely to be highly immunogenic, may prevent establishment of infection by *L. major* metacyclics transmitted by sand fly bite.

Leishmania show extensive developmental, strain, and species specific variation in LPG PG repeat structure, differences that play key roles in parasite transmission and vector competency (2). The methods used here for the *SCA* genes affecting developmental polymorphisms, or previously for the *SCG* genes affecting inter-specific polymorphisms, could readily be adapted to other *Leishmani*a where the requisite parasite species and lectin/antibody reagents exist. Notably, it will be particularly interesting to trace the occurrence of the different families of genes encoding LPG PG repeat-modifying activities during parasite evolution and adaptation to diverse sand fly vectors.

Acknowledgments—We thank Wandy Beatty for cryo-immunoelectron microscopy of GFP*SCA*1 transfectants, E. Fossman for help with GFP(*SCA*) fusion constructs, A. Garraway for help in TyK transposon mutagenesis, E. Handman for providing anti-GFP antibodies, G. Späth and A. Capul for assistance with fluorescence microscopy, P. Myler for permission to discusses cosmid sequences, and D. Sacks and R. Duncan and our laboratory members for discussions.

REFERENCES

1. Ashford, R. W., Desjeux, P., and deRaadt, P. (1992) *Parasitol. Today* **8,** 104–105
2. Sacks, D., and Kamhawi, S. (2001) *Annu. Rev. Microbiol.* **55,** 453–483
3. Sacks, D. L. (2001) *Cell Microbiol.* **3,** 189–196
4. Ilg, T. (2001) *Med. Microbiol. Immunol.* **190,** 13–17
5. Pimenta, P. F., Turco, S. J., McConville, M. J., Lawyer, P. G., Perkins, P. V., and Sacks, D. L. (1992) *Science* **256,** 1812–1815
6. Sacks, D. L., Brodin, T. N., and Turco, S. J. (1990) *Mol. Biochem. Parasitol.* **42,** 225–233
7. McConville, M. J., Turco, S. J., Ferguson, M. A., and Sacks, D. L. (1992) *EMBO J.* **11,** 3593–3600
8. Sacks, D. L. (1989) *Exp. Parasitol.* **69,** 100–103
9. Roditi, I., and Liniger, M. (2002) *Trends Microbiol.* **10,** 128–134
10. McConville, M. J., Schnur, L. F., Jaffe, C., and Schneider, P. (1995) *Biochem. J.* **310,** 807–818
11. Pimenta, P. F., Saraiva, E. M., Rowton, E., Modi, G. B., Garraway, L. A., Beverley, S. M., Turco, S. J., and Sacks, D. L. (1994) *Proc. Natl. Acad. Sci. U. S. A.* **91,** 9155–9156
12. Butcher, B. A., Turco, S. J., Hilty, B. A., Pimenta, P. F., Panunzio, M., and Sacks, D. L. (1996) *J. Biol. Chem.* **271,** 20573–20579
13. Sacks, D. L., Pimenta, P. F., McConville, M. J., Schneider, P., and Turco, S. J. (1995) *J. Exp. Med.* **181,** 685–697
14. Pimenta, P. F., Saraiva, E. M., and Sacks, D. L. (1991) *Exp. Parasitol.* **72,** 191–204
15. Sacks, D. L. (1992) *Infect Agents Dis.* **1,** 200–206
16. Ryan, K. A., Garraway, L. A., Descoteaux, A., Turco, S. J., and Beverley, S. M. (1993) *Proc. Natl. Acad. Sci. U. S. A.* **90,** 8609–8613
17. Descoteaux, A., Avila, H. A., Zhang, K., Turco, S. J., and Beverley, S. M. (2002) *EMBO J.* **21,** 4458–4469
18. Descoteaux, A., Luo, Y., Turco, S. J., and Beverley, S. M. (1995) *Science* **269,** 1869–1872
19. Beverley, S. M., and Turco, S. J. (1998) *Trends Microbiol.* **6,** 35–40
20. Dobson, D. E., Scholtes, L. D., Valdez, K. E., Sullivan, D. R., Mengeling, B. J., Cilmi, S., Turco, S. J., and Beverley, S. M. (2003) *J. Biol. Chem.* **278,** 15523–15531
21. Kapler, G. M., Coburn, C. M., and Beverley, S. M. (1990) *Mol. Cell. Biol.* **10,** 1084–1094
22. Sacks, D. L., Hieny, S., and Sher, A. (1985) *J. Immunol.* **135,** 564–569
23. Titus, R. G., Gueiros-Filho, F. J., de Freitas, L. A., and Beverley, S. M. (1995) *Proc. Natl. Acad. Sci. U. S. A.* **92,** 10267–10271
24. Ryan, K. A., Dasgupta, S., and Beverley, S. M. (1993) *Gene* (*Amst.*) **131,** 145–150
25. Sacks, D. L., and da Silva, R. P. (1987) *J. Immunol.* **139,** 3099–3106
26. Kelleher, M., Curtis, J. M., Sacks, D. L., Handman, E., and Bacic, A. (1994) *Mol. Biochem. Parasitol.* **66,** 187–200
27. Callahan, H. L., and Beverley, S. M. (1991) *J. Biol. Chem.* **266,** 18427–18430
28. Ha, D. S., Schwarz, J. K., Turco, S. J., and Beverley, S. M. (1996) *Mol. Biochem. Parasitol.* **77,** 57–64
29. Garraway, L. A., Tosi, L. R. O., Wang, Y., Moore, J. B., Dobson, D. E., and Beverley, S. M. (1997) *Gene* (*Amst.*) **198,** 27–35
30. Cunningham, M. L., and Beverley, S. M. (2001) *Mol. Biochem. Parasitol.* **113,** 199–213
31. Orlandi, P. A., Jr., and Turco, S. J. (1987) *J. Biol. Chem.* **262,** 10384–10391
32. Mahoney, A. B., Sacks, D. L., Saraiva, E., Modi, G., and Turco, S. J. (1999) *Biochemistry* **38,** 9813–9823
33. Ng, K., Handman, E., and Bacic, A. (1996) *Biochem. J.* **317,** 247–255
34. Mengeling, B. J., and Turco, S. J. (1999) *Anal. Biochem.* **267,** 227–233
35. Singer, S. J. (1990) *Annu. Rev. Cell Biol.* **6,** 247–296
36. Al-Qahtani, A., Teilhet, M., and Mensa-Wilmot, K. (1998) *Biochem. J.* **331,** 521–529
37. Unligil, U. M., and Rini, J. M. (2000) *Curr. Opin. Struct. Biol.* **10,** 510–517
38. Wiggins, C. A., and Munro, S. (1998) *Proc. Natl. Acad. Sci. U. S. A.* **95,** 7945–7950
39. Duncan, R., Alvarez, R., Jaffe, C. L., Wiese, M., Klutch, M., Shakarian, A., Dwyer, D., and Nakhasi, H. L. (2001) *Parasitol. Res.* **87,** 897–906
40. Turco, S. J., and Sacks, D. L. (1991) *Mol. Biochem. Parasitol.* **45,** 91–99
41. Ma, D., Russell, D. G., Beverley, S. M., and Turco, S. J. (1997) *J. Biol. Chem.* **272,** 3799–3805
42. Whitfield, C., and Valvano, M. A. (1993) *Adv. Microb. Physiol.* **35,** 135–246
43. Pelletier, I., and Sato, S. (2002) *J. Biol. Chem.* **277,** 17663–17670
44. Sacks, D. L., and Perkins, P. V. (1984) *Science* **223,** 1417–1419
45. Chakkalath, H. R., Siddiqui, A. A., Shankar, A. H., Dobson, D. E., Beverley, S. M., and Titus, R. G. (2000) *Infect. Immun.* **68,** 809–814
46. Guerra-Giraldez, C., Quijada, L., and Clayton, C. E. (2002) *J. Cell Sci.* **115,** 2651–2658
47. Schneider, P., McConville, M. J., and Ferguson, M. A. (1994) *J. Biol. Chem.* **269,** 18332–18337
48. Turco, S. J., and Descoteaux, A. (1992) *Annu. Rev. Microbiol.* **46,** 65–94